Giant enhancement of sum-frequency yield by surface-plasmon excitation

E. W. M. van der Ham,* Q. H. F. Vrehen, and E. R. Eliel[2]

Huygens Laboratory, Leiden University, P.O. Box 9504, 2300 RA Leiden, The Netherlands

V. A. Yakovlev, E. V. Alieva, L. A. Kuzik, and J. E. Petrov

Institute of Spectroscopy, Russian Academy of Sciences, Troitsk, Moscow region, 142092 Russia

V. A. Sychugov

General Physics Institute, Russian Academy of Sciences, Vavilova 38, Moscow, 117942, Russia

A. F. G. van der Meer

Stichting voor Fundamenteel Onderzoek der Materie (FOM) Institute for Plasma Physics Rijnhuizen, P.O. Box 1207, 3430 BE Nieuwegein, The Netherlands

Received September 11, 1998; revised manuscript received March 22, 1999

We show experimentally that the radiation generated in infrared–visible sum-frequency mixing at an air–silver interface can be greatly enhanced when the visible input beam excites a surface plasmon–polariton at the interface. With either a prism or a grating used to couple the visible radiation with the surface polariton, the sum-frequency-generation yield is observed to be enhanced by a factor of 10^2 for the prism and 10^4 for the grating for counterpropagating infrared and visible input beams. The result for the prism configuration can be simply understood in terms of the field enhancement associated with the surface polariton excited by the visible input beam. For the grating configuration there is an additional effect in that the nonlinear polarization at the sum frequency can also couple with a surface polariton. As a result the effective interaction length of the sum-frequency-mixing process is sizably increased. The experimental results are in good agreement with estimates based on this model. © 1999 Optical Society of America [S0740-3224(99)01907-4]

OCIS codes: 190.4350, 190.2620, 240.6680, 300.6420.

1. INTRODUCTION

In recent years second-order nonlinear optical methods have found widespread application in the study of surfaces and interfaces.[1–3] Second-harmonic generation and sum-frequency generation (SFG) have been favored for this application. Because SFG is technically more complicated than second-harmonic generation, the latter technique is much more widely used than SFG. For the study of molecular monolayers, however, SFG offers considerable advantages because the nonlinear optical process can rather easily be made resonant. Apart from the ensuing signal enhancement, the nonlinear optical process then also becomes molecule specific. In the experiment this is realized by the nonlinear optical process being driven with tunable IR radiation in combination with fixed-frequency visible radiation. The frequency of the IR radiation is then tuned across various vibrational modes of the molecules that make up the monolayer. The resulting specificity is of importance when different molecular species are present in the monolayer or when the supporting substrate participates in the nonlinear mixing process. Metals provide an example of such substrates.

The flux of photons that is generated at the new frequency (either the second-harmonic frequency or the sum frequency) is small because nonlinear optical processes are usually highly inefficient. In addition, the radiation at the new frequency is, for monolayers, generated by a sample with essentially zero depth. Nevertheless, even at submonolayer coverages second-harmonic generation and SFG can yield a detectable signal.[4] Yet in many cases there is a real need for an increased photon flux, particularly in SFG employing low-frequency vibrational modes of molecules in an adsorbed layer. This is illustrated by the fact that the sum-frequency activity of such modes is often vanishingly small even though the high-frequency vibrational modes are easily seen by SFG.[5]

Because of the risk of sample damage, the sum-frequency yield usually cannot be improved by increasing the flux density of the primary radiation. An attractive route is provided by methods in which the electromagnetic field at the sample interface is enhanced relative to the field of the incident radiation. Such enhancement occurs, for instance, in a total-internal-reflection geometry just beyond the angle for total internal reflection or in samples in which one excites a surface polariton.[6] Both these methods have been successfully employed in nonlinear optical experiments.[7–11] Whereas the total-internal-reflection geometry is being applied in some instances to SFG from adsorbed monolayers,[8–11] the possibilities of-

fered by the application of surface polaritons to SFG of interfacial layers have remained unexplored until recently. There exists, however, a long-standing connection between surface polaritons and second-order nonlinear optical methods, since these provide an elegant mechanism to optically excite surface modes of dielectric crystals.[12,13]

Recently we presented preliminary results regarding the increase of the sum-frequency yield from a bare silver film.[14] Enhancements ranging between 2 and 4 orders of magnitude were observed. In the present paper we report more extensive results on surface-polariton-aided SFG, comparing different modes of surface-polariton excitation, and we present a simple picture explaining the results.

2. SURFACE PLASMON–POLARITONS

The possibility that electromagnetic waves can propagate on a surface or interface was first discussed by Sommerfeld in the context of the propagation of radio waves.[15] These solutions to Maxwell's equations exist under well-defined conditions regarding the dielectric functions $\epsilon_a(\omega)$ and $\epsilon_b(\omega)$ of the media above ($z > 0$) and below ($z < 0$) the interface; either $\mathrm{Re}(\epsilon_a(\omega)) < 0$ and $|\mathrm{Re}(\epsilon_a(\omega))| > \mathrm{Re}(\epsilon_b(\omega))$ or $\mathrm{Re}(\epsilon_b(\omega)) < 0$ and $|\mathrm{Re}(\epsilon_b(\omega))| > \mathrm{Re}(\epsilon_a(\omega))$. The electric field is p polarized and can be written as

$$\mathbf{E}^a(\omega) = [E_x{}^a(\omega)\mathbf{x} + E_z{}^a(\omega)\mathbf{z}] \times \exp(-\alpha_a{}^\omega z - \imath\omega t + \imath K_{\mathrm{SPP}}{}^\omega x), \quad (1)$$

$$\mathbf{E}^b(\omega) = [E_x{}^b(\omega)\mathbf{x} + E_z{}^b(\omega)\mathbf{z}] \times \exp(-\alpha_b{}^\omega z - \imath\omega t + \imath K_{\mathrm{SPP}}{}^\omega x), \quad (2)$$

where the surface excitation propagates along the x direction. Because of the continuity of the tangential component of the electric field and the normal component of the displacement field, one has $E_x{}^a(\omega) = E_x{}^b(\omega)$ and $E_z{}^a(\omega) = (\epsilon_b(\omega)/\epsilon_a(\omega))E_z{}^b(\omega)$. On both sides of the interface the amplitude of the wave decays away from the interface with the decay constant

$$\alpha_i{}^\omega = \left[(K_{\mathrm{SPP}}{}^\omega)^2 - \epsilon_i(\omega)\left(\frac{\omega}{c}\right)^2\right]^{1/2}, \qquad i \in (a, b). \quad (3)$$

The (complex) propagation constant of the surface wave is given by

$$K_{\mathrm{SPP}}{}^\omega \equiv K^\omega + \imath\kappa^\omega = \frac{\omega}{c}\left[\frac{\epsilon_a(\omega)\epsilon_b(\omega)}{\epsilon_a(\omega) + \epsilon_b(\omega)}\right]^{1/2}, \quad (4)$$

with $K^\omega > \omega/c$.

In the present case we employ surface waves propagating along the interface between vacuum and a metal at frequencies well below the metal's plasma frequency ω_P. Hence $\epsilon_a(\omega) = 1$ and $\epsilon_b(\omega) \equiv \epsilon_b{}'(\omega) + \imath\epsilon_b{}''(\omega)$ is complex with $\epsilon_b{}'(\omega) < 0$ and $|\epsilon_b{}'(\omega)| > \epsilon_a(\omega)$. A surface wave along such an interface is called a surface plasmon–polariton (SPP). For $\omega \ll \omega_P$ one has $|\epsilon_b{}'(\omega)| \gg |\epsilon_b{}''(\omega)|$ and $|\epsilon_b{}'(\omega)| \gg \epsilon_a(\omega)$; in this case one can approximate the expressions for $\alpha_a{}^\omega$ and $\alpha_b{}^\omega$ as[16]

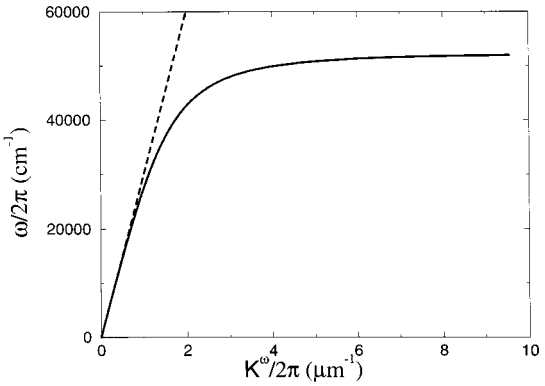

Fig. 1. Dispersion relation of a SPP propagating along the interface between vacuum and a metal (solid curve). The dashed line shows the dispersion relation of free-space electromagnetic radiation.

$$\alpha_a{}^\omega \approx \frac{\omega}{c}\left[\frac{-1}{1 + \epsilon_b{}'(\omega)}\right]^{1/2}, \quad (5)$$

$$\alpha_b{}^\omega \approx |\epsilon_b{}'(\omega)|\alpha_a{}^\omega. \quad (6)$$

The propagation constant K^ω and damping coefficient κ^ω of the SPP can be written as[16]

$$K^\omega \approx \frac{\omega}{c}\left\{\frac{\epsilon_b{}'(\omega)}{1 + \epsilon_b{}'(\omega)} + \frac{\epsilon_b{}''(\omega)^2}{[1 + \epsilon_b{}'(\omega)]^3}\right\}^{1/2}, \quad (7)$$

$$\kappa^\omega \approx \frac{\omega}{2c}\frac{\epsilon_b{}''(\omega)}{\{\epsilon_b{}'(\omega)[\epsilon_b{}'(\omega) + 1]^3\}^{1/2}}. \quad (8)$$

The dispersion relation of the SPP along such an interface is shown in Fig. 1 (solid curve) together with that of electromagnetic radiation in free space. The figure directly shows the wave-vector mismatch between a SPP and free-space radiation at the same frequency. Because of this mismatch some element is necessary to couple free-space radiation with a SPP at a metal–vacuum interface.

3. EXPERIMENTAL METHOD

The sum-frequency spectrometer that is used in the present experiment has been discussed in some detail in Refs. 17–19. Briefly, wavelength tunable ($5 < \lambda_{\mathrm{ir}} < 110\,\mu$m) IR radiation from the FELIX free-electron laser[20] is mixed at the surface of a silver film with the output of a fixed-frequency (λ_{vis}=523.5 nm) visible laser system. Both lasers generate bursts (≈5 μs long) of synchronized, short, powerful pulses that overlap temporally and spatially on the sample. In the present experiment FELIX delivers pulses of ≈1 ps in duration with an energy content of 2 μJ at a 1-GHz repetition rate while the visible laser yields pulses of ≈7 ps in duration with an energy of 4 μJ at a repetition rate of 250 MHz. Both laser beams are p polarized. The generated sum-frequency radiation is emitted as a collimated beam and is focused on a liquid-nitrogen-cooled CCD camera that serves as a detector. A narrow-band interference-filter set with a compound transmission of ≈50% at the sum frequency is used to suppress stray light at the visible input wavelength. In the experiment the IR wavelength is fixed at $\lambda_{\mathrm{ir}} = 10.0\,\mu$m.

We study SPP-aided SFG at the interface between air and a silver film with the SPP excited by the visible input radiation. The SPP becomes resonantly excited when the component of the wave vector of the incident visible radiation parallel to the interface matches the wave vector K^{vis} of the SPP at that frequency. Two approaches are employed to realize this matching: a fused-silica prism in the Kretschmann configuration[21] and a grating structure in the silver film.

In both experiments involving prism and grating coupling the SFG yield is measured as a function of the angle of incidence of the visible input radiation. In addition, we measure the reflectivity of the sample as a function of this angle. The latter provides us with a measure of the efficiency of SPP excitation.[6] The angle subtended by the two input beams remains constant during all experiments. For the prism setup this angle is approximately 170°, and for the grating setup approximately 91°.

A. Surface-Plasmon–Polariton Excitation with Prism

For these measurements we employ a 90° fused-silica prism with a 50-nm-thick silver film on the hypotenuse (see Fig. 2). Wave-vector matching at the air–silver interface is achieved by our choosing the appropriate angle of incidence θ_{vis} of the visible input radiation:

$$K^{\mathrm{vis}} = n(\omega_{\mathrm{vis}})\frac{\omega_{\mathrm{vis}}}{c}\sin\theta_{\mathrm{vis}}, \tag{9}$$

where $n(\omega_{\mathrm{vis}})$ is the refractive index of fused silica at frequency ω_{vis}.

The infrared radiation comes in from the opposite side (see Fig. 2). The radiation at the sum frequency is emitted into the fused silica in a direction that is somewhat different from that of the specularly reflected visible input beam. The wave vector of the sum-frequency radiation has a component along the interface given by

$$\begin{aligned}|k_x(\omega_{\mathrm{sfg}})| &= n(\omega_{\mathrm{sfg}})\frac{\omega_{\mathrm{sfg}}}{c}\sin\theta_{\mathrm{sfg}} \\ &= n(\omega_{\mathrm{vis}})\frac{\omega_{\mathrm{vis}}}{c}\sin\theta_{\mathrm{vis}} - \frac{\omega_{\mathrm{ir}}}{c}\sin\theta_{\mathrm{ir}},\end{aligned} \tag{10}$$

where $n(\omega_{\mathrm{sfg}})$ is the refractive index of fused silica at the sum frequency and θ_{sfg} the angle of emission of the generated sum-frequency radiation. The minus sign in Eq. (10) arises because the input fields are counterpropagating; in a copropagating configuration this becomes a plus sign.

B. Surface-Plasmon–Polariton Excitation with Grating

The substrate for this series of measurements is a flat glass plate containing the grating structure at its surface. The grating (groove period $a = 301$ nm, groove depth 15–20 nm) is written by photolithographic techniques and subsequent ion etching. The substrate is overcoated with a 200-nm-thick silver film, made by thermal evaporation in a vacuum chamber.

To resonantly excite the SPP, the visible input beam has to come in at the proper angle of incidence in this case, also:

$$K^{\mathrm{vis}} = k_x(\omega_{\mathrm{vis}}) \pm N k_{\mathrm{grating}} \tag{11}$$

$$= \frac{\omega_{\mathrm{vis}}}{c}\sin\theta_{\mathrm{vis}} \pm N\frac{2\pi}{a}, \tag{12}$$

where N is the diffraction order. Here $k_x(\omega_{\mathrm{vis}})$ is the component of the wave vector of the visible input beam along the sample and $k_{\mathrm{grating}} = 2\pi/a$.

With $\lambda_{\mathrm{vis}} = 523.5$ nm, a polariton is excited when $\theta_{\mathrm{vis}} \approx 43.5°$ and $N = -1$. The SPP is then counterpropagating with the visible input beam (see Fig. 2) and $K^{\mathrm{vis}} = k_x(\omega_{\mathrm{vis}}) - k_{\mathrm{grating}}$. In the chosen geometry the SPP is then codirectional with the IR input beam. The nonlinear polarization at the sum frequency $\tilde{\mathbf{P}}^{(2)}(\mathbf{r}, t)$ is given by

$$\tilde{\mathbf{P}}^{(2)}(\mathbf{r}, t) = \mathbf{P}^{(2)}(\omega_{\mathrm{sfg}})\delta(z)\exp[\imath k_x^{\mathrm{NL}}(\omega_{\mathrm{sfg}})x - \imath\omega_{\mathrm{sfg}}t], \tag{13}$$

where $\mathbf{P}^{(2)}(\omega_{\mathrm{sfg}})$ is the nonlinear surface polarization of the air–metal interface. Its wave vector is given by

$$k_x^{\mathrm{NL}}(\omega_{\mathrm{sfg}}) = K^{\mathrm{vis}} + k_x(\omega_{\mathrm{ir}}), \tag{14}$$

where $k_x(\omega_{\mathrm{ir}})$ is the component of the wave vector of the IR input radiation parallel to the interface. In the present configuration we have (see below) $|k_x^{\mathrm{NL}}(\omega_{\mathrm{sfg}})|$

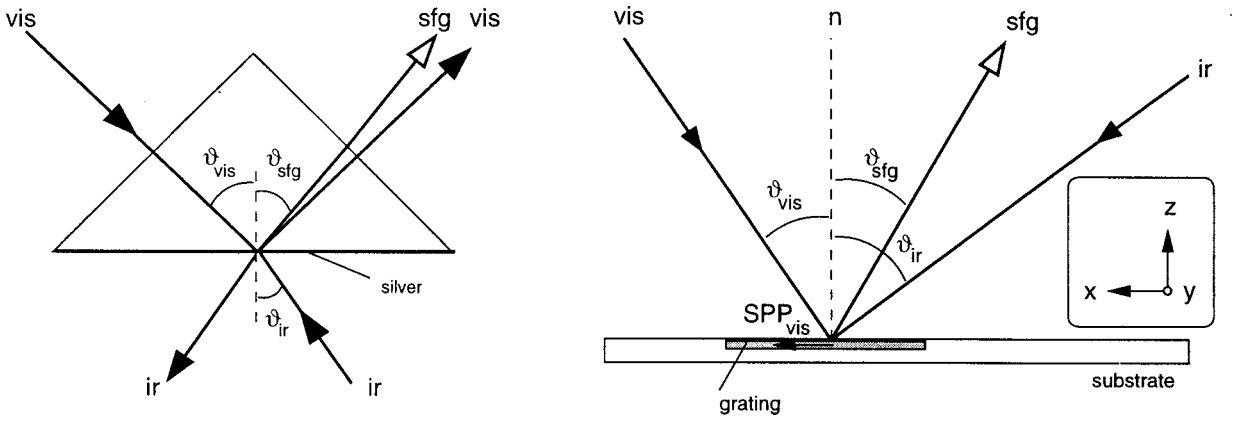

Fig. 2. Configurations for SFG with a SPP at the visible input wavelength. Left, configuration of input beams used with the prism; the SPP travels to the right, counterdirectional to the IR input beam. Right, configuration used with the grating; the SPP at the visible input wavelength is codirectional with the IR input beam.

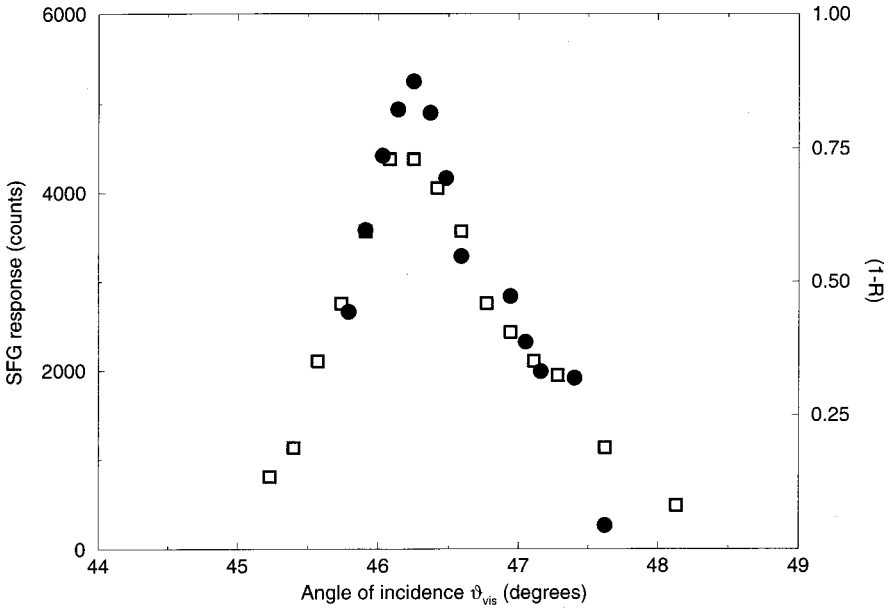

Fig. 3. Experimental results for the sum-frequency yield obtained with the prism coupler (filled symbols, scale at left). The open symbols show the fraction of the visible input power that is coupled into a polariton (scale at right).

$> \omega_{sfg}/c$; hence this nonlinear polarization cannot radiate into free space. Sum-frequency radiation is, however, emitted in a direction determined by

$$k_x(\omega_{sfg}) = k_x^{NL}(\omega_{sfg}) + k_{grating} \quad (15)$$

$$= k_x(\omega_{vis}) + k_x(\omega_{ir}) \quad (16)$$

$$= \frac{\omega_{vis}}{c}\sin\theta_{vis} - \frac{\omega_{ir}}{c}\sin\theta_{ir}, \quad (17)$$

i.e., exactly in the direction in which the sum-frequency radiation from a noncorrugated interface is emitted for counterpropagating input beams. There is thus a unique propagation direction of the sum-frequency radiation, whether or not the input beams overlap with the grating and one couples into the SPP. This makes a comparison between SPP-aided and non-SPP-aided SFG simple for a grating coupler because one can switch from one to the other simply by moving the sample relative to the input beams.

4. RESULTS AND DISCUSSION

The results for the prism configuration are shown in Fig. 3. The dots represent the measured values of the sum-frequency yield from the air–silver interface as a function of the angle of incidence of the visible radiation. The squares show the quantity $(1 - R)$, representing the fraction of the incident visible-beam energy that is coupled into the surface plasmon (R is the measured reflectivity of the sample). At resonance ($\theta_{vis} \approx 46.3°$) this fraction reaches a maximum at a value equal to 0.72, indicating that a large fraction of the incident beam energy is coupled into the SPP. The variation of the sum-frequency yield and of $(1 - R)$ with the angle of incidence have very similar shape, demonstrating that the increase of the sum-frequency response is really the result of the surface-plasmon excitation. Both resonances have a width of roughly 1°, a value that is characteristic for the response of a 50-nm-thick silver film when a well-collimated beam at the visible input wavelength is employed. At resonance the sum-frequency yield is larger by approximately a factor of 100 as compared with the yield far off resonance. One can define a field-enhancement factor for the surface polariton given by

$$\gamma_{vis} = \frac{E_{SPP}(\omega_{vis})}{E_0(\omega_{vis})}, \quad (18)$$

where $E_{SPP}(\omega_{vis})$ is the electric field strength associated with the polariton [see Eq. (1)] and $E_0(\omega_{vis})$ is the field strength of the input radiation. For the Kretschmann configuration one calculates $\gamma_{vis}^2 \approx 100$,[22,23] in excellent agreement with the enhancement of the sum-frequency yield. Clearly, the observed increase in the sum-frequency yield can be explained in terms of the enhancement of the visible input field.

With grating excitation of the SPP the sum-frequency yield off the air–silver interface is considerably larger than that obtained in the prism configuration.[14] For various gratings with slightly different grating parameters we find the SFG yield to be increased by a factor of 10^3–10^4. Here the enhancement factor is found by comparing the SPP-aided SFG yield with the yield obtained away from the grating. We ascertained that all of the enhancement is SPP induced by performing a measurement in which the wave vector of the grating is aligned perpendicular to the plane of incidence. In this configuration—which usually does not lead to excitation of an SPP (see, however, Ref. 24)—the sum-frequency yield is not enhanced. The fact that this yield is almost exactly equal to that found when the input beams do not overlap with the grating indicates that the surface roughness of the grating does not give rise to signal enhancement.

The field enhancement of the visible input field for the grating configuration can be simply expressed in terms of

the power-coupling efficiency η, the inverse attenuation length $(\alpha_a{}^{\mathrm{vis}})^{-1}$ of the field normal to the air–silver interface [see Eq. (5)], and the damping coefficient κ^{vis} [see Eq. (8)] of the surface polariton. As the spot size of the visible beam on the sample is considerably larger than the damping length of the polariton $(2\kappa^{\mathrm{vis}})^{-1}$, the enhancement is given by[25]

$$\gamma_{\mathrm{vis}}{}^2 = \left[\frac{E_{\mathrm{SPP}}(\omega_{\mathrm{vis}})}{E_0(\omega_{\mathrm{vis}})}\right]^2 = \eta \cos\theta_{\mathrm{vis}} \frac{\alpha_a{}^{\mathrm{vis}}}{\kappa^{\mathrm{vis}}}. \tag{19}$$

At the visible input wavelength ($\lambda_{\mathrm{vis}} = 0.5235\,\mu\mathrm{m}$) we have for the silver film[26] $[\epsilon_b(\omega_{\mathrm{vis}})]^{1/2} = 0.05 + \iota 3.324$, yielding $\alpha_a{}^{\mathrm{vis}} \approx 3.78\,\mu\mathrm{m}^{-1}$ and $\kappa^{\mathrm{vis}} \approx 0.0188\,\mu\mathrm{m}^{-1}$. Together with an estimated coupling efficiency $\eta \approx 1$, this yields $\gamma_{\mathrm{vis}}{}^2 \approx 150$, much less than the enhancement factor found in the experiment.

The experimental enhancement factor thus cannot be understood only in terms of the increase of the visible input field and, consequently, of the driving nonlinear polarization at the sum frequency. This is not surprising in view of the fact that this nonlinear polarization cannot radiate directly into free space, as mentioned earlier. To substantiate the latter statement, we calculate the relevant wave vectors [see Eqs. (7) and (14)]. The real part of the propagation constant of the polariton at $2\pi c/\omega_{\mathrm{vis}} = 0.5235\,\mu\mathrm{m}$ is given by $K^{\mathrm{vis}} = 2\pi/0.4992\,\mu\mathrm{m}^{-1}$. The component of the wave vector of the nonlinear surface polarization along the interface then equals $k_x{}^{\mathrm{NL}}(\omega_{\mathrm{sfg}}) = 2\pi/0.4815\,\mu\mathrm{m}^{-1}$ for $\lambda_{\mathrm{ir}} = 10.0\,\mu\mathrm{m}$ and $\theta_{\mathrm{ir}} = 47.5°$. The free-space wave vector of the generated sum frequency has the length $\omega_{\mathrm{sfg}}/c = 2\pi/0.4975\,\mu\mathrm{m}^{-1}$; thus $|k_x{}^{\mathrm{NL}}(\omega_{\mathrm{sfg}})| > \omega_{\mathrm{sfg}}/c$. Because of this inequality, a free-space radiative solution of the wave equation is not allowed.

The wave equation for the field at the sum-frequency, however, has a solution in the form of a surface polariton. These solutions to the wave equation are known to have increased field strength, displaying resonant enhancement when there is wave vector matching between the surface polariton at the sum frequency and the driving nonlinear polarization.[7,27] The propagation constant of the polariton at the sum frequency can be written as

$$K_{\mathrm{SPP}}{}^{\mathrm{sfg}} = K^{\mathrm{sfg}} + \iota\kappa^{\mathrm{sfg}}, \tag{20}$$

where K^{sfg} and κ^{sfg} are calculated from Eqs (7) and (8), given the value of $\epsilon_b(\omega_{\mathrm{sfg}})$. In general there is a mismatch $\Delta k(\omega_{\mathrm{sfg}}) \equiv |K^{\mathrm{sfg}} - k_x{}^{\mathrm{NL}}(\omega_{\mathrm{sfg}})|$ between the wave vector K^{sfg} of the polariton at the sum frequency and the wave vector of the driving nonlinear polarization $k_x{}^{\mathrm{NL}}(\omega_{\mathrm{sfg}})$, limiting the resonant enhancement.

The generation of a surface polariton at the sum frequency by the nonlinear surface polarization is very similar to SFG in the bulk or in waveguides for the case in which the propagation vectors of the driving nonlinear polarization and of the generated field point in exactly the same direction. This situation gives rise to coherent buildup of the field at the sum frequency over a length equal to the coherence length,

$$\ell_c \equiv \{[\Delta k(\omega_{\mathrm{sfg}})]^2 + (\kappa^{\mathrm{sfg}})^2\}^{-1/2}, \tag{21}$$

with $\Delta k(\omega_{\mathrm{sfg}})$ the phase mismatch and κ^{sfg} the field-attenuation coefficient of the surface polariton at the sum frequency. For the present experiment we have, with $\epsilon_b(\omega_{\mathrm{sfg}}) = -9.564 + \iota 0.309$ (see Ref. 26), $K^{\mathrm{sfg}} = 2\pi/0.4707\,\mu\mathrm{m}^{-1}$, $\Delta k(\omega_{\mathrm{sfg}}) = 0.298\,\mu\mathrm{m}^{-1}$, and $\kappa^{\mathrm{sfg}} = 0.025\,\mu\mathrm{m}^{-1}$. Since $\Delta k(\omega_{\mathrm{sfg}}) \gg \kappa^{\mathrm{sfg}}$, we have $\ell_c \approx [\Delta k(\omega_{\mathrm{sfg}})]^{-1} = 3.4\,\mu\mathrm{m}$, dominated by the phase mismatch.

To quantify the sum-frequency yield in the present configuration, as compared with that in which none of the input beams couples with a surface polariton, one has to take three factors into account. First, the field enhancement γ_{vis} of Eq. (19) leads directly to an equally large enhancement of the driving nonlinear surface polarization. Second, this nonlinear surface polarization excites a surface polariton, resulting in a very large increase of the effective generation length. This factor equals ℓ_c/Δ, where ℓ_c is the coherence length and Δ the effective thickness (<1 nm) of the layer in the metal[28] that contributes to the sum-frequency response. Third, one has to take into account the spatial overlap between the field that is to be generated and the nonlinear surface polarization.[27] Because the nonlinear surface polarization is confined to a layer that is very thin compared with the spatial extent $(\alpha_a{}^{\mathrm{sfg}})^{-1}$ of the SPP, this overlap is rather small, yielding a factor of order $\alpha_a{}^{\mathrm{sfg}}\Delta$. Taking everything together, we estimate the sum-frequency yield to be increased by a factor

$$G = \gamma_{\mathrm{vis}}{}^2(\ell_c/\Delta)^2(\alpha_a{}^{\mathrm{sfg}}\Delta)^2 = \gamma_{\mathrm{vis}}{}^2(\ell_c\alpha_a{}^{\mathrm{sfg}})^2 \approx 2.5 \times 10^4. \tag{22}$$

This estimate for the gain factor G is in satisfactory agreement with the values found in the experiment, the more so in view of the approximations that have been made. For instance, the processes of SPP incoupling and outcoupling, damping, and the nonlinear generation process are discussed as separate phenomena. In reality, of course, all these processes take place simultaneously. Obviously, this has to be taken into account when the en-

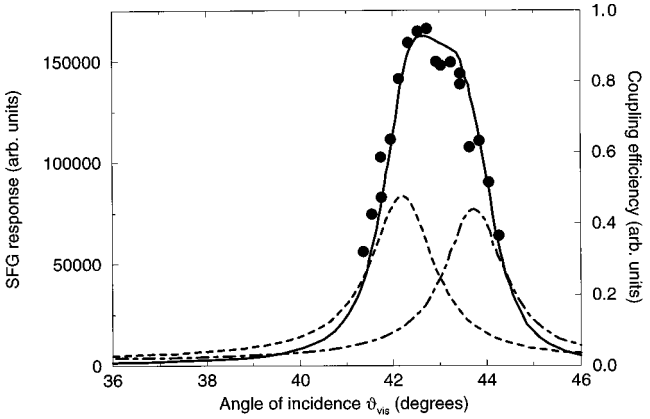

Fig. 4. Experimental results (filled symbols) for the sum-frequency yield on top of the visible grating as a function of the angle of incidence of the visible input radiation. The dotted–dashed curve shows the excitation efficiency of the polariton at the visible input wavelength (input coupling), and the dashed curve displays the phase matching between the nonlinear polarization and the polariton at the sum frequency. The solid curve gives the product of these two factors scaled to the experimental results.

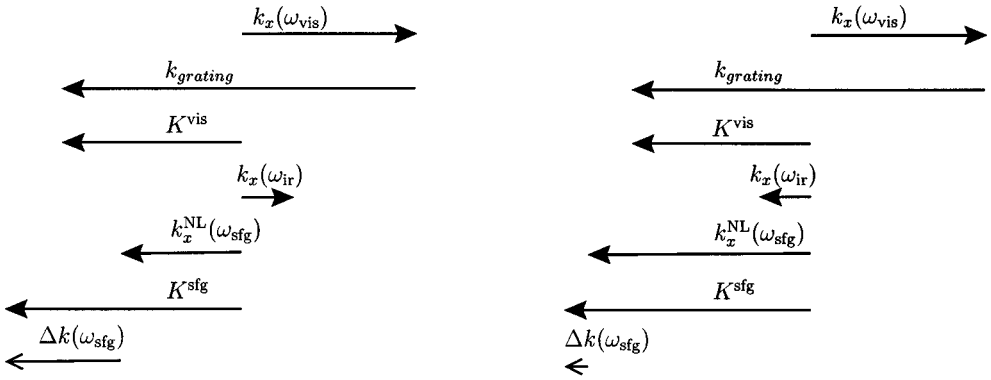

Fig. 5. Wave-vector components parallel to the interface for the grating coupler for (right) counterpropagating and (left) copropagating configurations of the input beams. The bottom arrows indicate the wave-vector mismatch for the respective cases.

hancement factor is calculated more quantitatively. Of particular importance here is the question of whether the outcoupling does not destroy the coherent buildup of the sum-frequency field.

The values of the parameters all apply to an angle of incidence for which the surface polariton at the visible input frequency is optimally excited ($\theta_{vis} = 43.5°$). At this angle the wave-vector mismatch $\Delta k(\omega_{sfg})$ is rather large. When the sample is rotated in such a way that the angle of incidence is modified, the coupling with the surface polariton at the visible input frequency deteriorates. However, the wave-vector mismatch at the sum frequency $\Delta k(\omega_{sfg})$ may become smaller in the process, thereby improving the nonlinear generation process. This is actually the case here, as is shown in Fig. 4. Here the dashed–dotted curve shows the excitation probability (basically $\gamma_{vis}{}^2$) of the SPP at the visible input wavelength as a function of θ_{vis}; it peaks at $\theta_{vis} = 43.5°$ and has a width determined by κ^{vis}. The dashed curve shows the variation of the efficiency of the nonlinear generation process that is due to the coupling with the SPP at the sum frequency for a given nonlinear surface polarization (basically $\ell_c{}^2$). The SFG enhancement factor is given by the product of these two factors [see Eq. (22)]; it is displayed as the solid curve in Fig. 4. The latter is scaled to the experimental data for the SFG yield, shown as dots. The agreement between the solid curve and the experimental data is excellent, which shows that the enhancement factor is well understood.

With the grating coupler we also used a copropagating arrangement of the input beams (in contrast to the experiment discussed above). In the copropagating setup we find the sum-frequency yield to be enhanced by a factor of the order of 100 under optimal coupling conditions. In this configuration the wave-vector mismatch $\Delta k(\omega_{sfg})$ at optimal incoupling is substantially larger than that for the counterpropagating setup (see Fig. 5). When the sample is oriented such that the wave-vector mismatch vanishes, the visible input radiation can no longer couple efficiently with a SPP. Therefore only a single enhancement factor comes into play for the grating coupler in a copropagating configuration.

The situation is quite similar for the prism coupler, except that the role of the copropagating and counterpropagating geometries are interchanged. For the counterpropagating geometry we find, as discussed above, that field enhancement of the input wave is all that comes into play. Coherent buildup of the sum-frequency field is precluded because $k_x{}^{NL}(\omega_{sfg}) = K^{vis} - k_x(\omega_{ir})$ and $k_x{}^{NL}(\omega_{sfg}) < n(\omega_{sfg})\omega_{sfg}/c$: The nonlinear polarization can directly radiate into the prism. In a copropagating arrangement $k_x{}^{NL}(\omega_{sfg}) = K^{vis} + k_x(\omega_{ir})$ and $k_x{}^{NL}(\omega_{sfg}) > n(\omega_{sfg})\omega_{sfg}/c$. The nonlinear polarization cannot radiate into free space and has to couple with a SPP at the sum frequency. Hence for a prism coupler in a copropagating setup one expects an enhancement of the sum-frequency yield similar to that attained with the grating in a counterpropagating configuration. We have been able to confirm this experimentally. It has, however, not been possible to record the full angular dependence of the sum-frequency yield for the prism coupler in a copropagating arrangement of input beams because the radiation at the sum-frequency is not easily separated from that of the reflected visible input beam (for $\lambda_{ir} = 10.0\ \mu$m).

5. CONCLUSIONS

In this study of visible-SPP-assisted infrared–visible sum-frequency generation we have shown that, without great effort, the sum-frequency yield can be enormously enhanced. In configurations involving prism and grating coupling with counterpropagating input beams we have achieved an increase of the sum-frequency response by 2–4 orders of magnitude. The 2 orders of magnitude, observed in the experiment with the prism coupler, are explained in terms of the field-enhancement associated with the concentrating effect that is due to the excitation of a surface polariton. To explain the even larger effects associated with the employed grating configuration, an additional mechanism is invoked. It involves coupling with a surface polariton at the sum frequency, giving rise to a substantial increase of the effective interaction length of the nonlinear optical process. We have also shown that for a copropagating arrangement of the input beams similar enhancement factors are found. In that case the enhancement factor is largest for the prism coupler.

Because of the orders-of-magnitude increase in signal yield, SPP-aided SFG holds great promise for sum-frequency spectroscopy of overlayers on top of metals.[29] An additional appealing aspect is that the SPP enhance-

ment combines well with the self-dispersive method for sum-frequency spectroscopy.[18,19]

ACKNOWLEDGMENTS

This work was supported by the Technology Foundation (STW), the Stichting voor Fundamenteel Onderzoek der Materie (FOM), and the Russian Foundation for Fundamental Research under grant 97-02-16792. We highly appreciate the skillful assistance of the FELIX staff and gratefully acknowledge A. G. Mal'shukov and G. Knippels for stimulating discussions. Finally, we thank I. F. Salakhtudinov for help with the sample preparation.

*Present address, Nederlands Meetinstituut, P.O. Box 654, 2600 AR Delft, The Netherlands.

[2]E. R. Eliel's e-mail address is eliel@molphys.leidenuniv.nl.

REFERENCES

1. Y. R. Shen, Nature (London) **337**, 519 (1989).
2. J. F. McGilp, D. Weaire, and C. H. Patterson, *Epioptics, Linear and Nonlinear Optical Spectroscopy of Surfaces and Interfaces* (Springer-Verlag, Berlin, 1995).
3. P.-F. Brevet, *Surface Second Harmonic Generation* (Presses Polytechniques et Universitaires Romande, Lausanne, 1997).
4. T. F. Heinz, C. K. Chen, D. Ricard, and Y. R. Shen, Phys. Rev. Lett. **48**, 478 (1982).
5. R. Braun, B. D. Casson, C. D. Bain, E. W. M. van der Ham, Q. H. F. Vrehen, E. R. Eliel, A. M. Briggs and P. B. Davies, J. Chem. Phys. **110**, 4634 (1999).
6. G. N. Zhizhin, M. A. Moskalova, E. V. Shomina, and V. A. Yakovlev, in *Surface Polaritons*, V. M. Agranovich and D. L. Mills, eds. (North-Holland, Amsterdam, 1982), Chap. 3.
7. Y. R. Shen, Phys. Rep. **194**, 303 (1990).
8. S. R. Hatch, R. S. Polizotti, S. Dougal, and P. Rabinowitz, Chem. Phys. Lett. **196**, 97 (1992).
9. J. C. Conboy, J. L. Daschbach, and G. L. Richmond, J. Phys. Chem. **98**, 9688 (1994).
10. J. C. Conboy, M. C. Messmer, and G. L. Richmond, J. Phys. Chem. **100**, 7617 (1996).
11. J. Löbau and K. Wolfrum, J. Opt. Soc. Am. B **14**, 2505 (1997).
12. D. N. Mirlin, in *Surface Polaritons*, V. M. Agranovich and D. L. Mills, eds. (North-Holland, Amsterdam, 1982), Chap. 1.
13. Y. R. Shen and F. de Martini, in *Surface Polaritons*, V. M. Agranovich and D. L. Mills, eds. (North-Holland, Amsterdam, 1982), Chap. 14.
14. E. V. Alieva, Y. E. Petrov, V. A. Yakovlev, E. R. Eliel, E. W. M. van der Ham, Q. H. F. Vrehen, A. F. G. van der Meer, and V. A. Sychugov, JETP Lett. **66**, 609 (1997).
15. A. Sommerfeld, Ann. Phys. (Leipzig) **4**, 665 (1909).
16. C. A. Ward, R. J. Bell, R. W. Alexander, G. S. Kovener, and I. Tyler, Appl. Opt. **13**, 2378 (1974).
17. E. R. Eliel, E. W. M. van der Ham, Q. H. F. Vrehen, G. W. 't Hooft, M. Barmentlo, J. M. Auerhammer, A. F. G. van der Meer, and P. W. van Amersfoort, Appl. Phys. A: Solids Surf. **60**, 113 (1995).
18. E. W. M. van der Ham, Q. H. F. Vrehen, and E. R. Eliel, Opt. Lett. **21**, 1448 (1996).
19. E. W. M. van der Ham, Q. H. F. Vrehen, and E. R. Eliel, Surf. Sci. **398**, 96 (1996).
20. D. Oepts, A. F. G. van der Meer, and P. W. van Amersfoort, Infrared Phys. **36**, 297 (1995).
21. E. Kretschmann, Z. Phys. **241**, 313 (1971).
22. W. N. Hansen, J. Opt. Soc. Am. **58**, 380 (1968).
23. B. Pettinger, A. Tadjeddine, and D. M. Kolb, Chem. Phys. Lett. **66**, 544 (1979).
24. R. A. Watts, T. W. Preist, and J. R. Sambles, Phys. Rev. Lett. **79**, 3978 (1997).
25. I. A. Avrutsky, P. V. Basakutsa, and S. Surov, *Waveguide Corrugated Structures in Integrated and Fiber Optics* (Nauka, Moscow, 1991).
26. P. B. Johnson and R. W. Christy, Phys. Rev. B **6**, 4370 (1972).
27. Y. R. Shen, *The Principles of Nonlinear Optics* (Wiley, New York, 1984).
28. J. Rudnick and E. A. Stern, Phys. Rev. B **4**, 4274 (1971).
29. E. V. Alieva, L. Kuzik, and V. A. Yakovlev, Chem. Phys. Lett. **292**, 542 (1998).